LASER PULSE SHAPING VIA ITERATIVE LEARNING CONTROL AND INFINITE-DIMENSIONAL EXTREMUM SEEKING

Beibei Ren[*], **Paul Frihauf, Miroslav Krstic**
Department of Mechanical and Aerospace Engineering
University of California
San Diego, California 92093
Email: helenren.ac@gmail.com, pfrihauf@ucsd.edu, krstic@ucsd.edu

Robert J. Rafac
Cymer Inc.
San Diego, Cafornia, 92127
Email: Robert_Rafac@cymer.com

ABSTRACT

We investigate pulse shaping and optimization for a laser amplifier. Due to the complex character of the nonlinear PDE dynamics involved in the laser model, it is of interest to consider non-model based methods for pulse shaping. We determine input pulse shapes for an unknown laser dynamics model using iterative learning control (ILC) and infinite-dimensional extremum seeking (ES), which is a real-time optimization strategy. We utilize ILC to obtain the input pulse shape that generates a desired output pulse shape and ES to find the input pulse that maximizes the energy amplifier gain. Both single-pass and double-pass laser models are investigated. The effectiveness of these approaches is illustrated via numerical simulations.

INTRODUCTION

Control of the shape of laser pulses is a key problem in photolithography light sources, where fundamental physics and control theory come together. The goals are to provide a stable output characteristic (pulse-to-pulse consistency and robustness to manufacturing tolerances, thermal effects, and mild optical damage), extract maximum stored energy from the amplifier gain medium with minimum input signal, and minimize the sensitivity of the total (integrated over a pulse period) output energy to total input energy. Some of these objectives may be competing, which calls not only for feedback design techniques but also for real-time optimization techniques.

In [1], the growth of a radiation pulse in a laser amplifier was described by nonlinear, time-dependent photon transport equations, which account for the effect of the radiation on the medium as well as vice versa. In [2], a one-dimensional model including Poisson's equation to consider the space-charge for a discharge-excited ArF excimer laser has been developed. Due to the complex character of the nonlinear partial differential equation (PDE) dynamics involved, it is of interest to consider non-model based methods for pulse shaping.

The operation of light sources for lithography is inherently repetitive. Exploiting the periodic nature of the process and its corresponding control actions can be done effectively by incorporating iterative learning control (ILC) methodologies into the light source design. ILC is a control methodology that improves system performance over repeated trials and has become a well-established field with many successful theoretical results and applications that range from robotics to hard disk drives [3–5]. However, there are only a few works [6, 7], which apply ILC to distributed parameter systems governed by PDEs. In this paper, we adopt the proportional-differential-type (PD-type) ILC scheme for pulse shaping of the laser amplifier system with the output pulse shape given, where the spatio-temporal evolution of irradiance and excimer population in a laser amplifier, is governed by a coupled nonlinear first-order hyperbolic PDE and a nonlinear ordinary differential equation (ODE) (extended from the classical model [1]).

Numerous optimization problems exist in the design and real-time operation of light sources for photolithography. One of them, which is pursued in this paper, is pulse shape optimization. Extremum seeking (ES) [8] is employed in this work to design the finite-time optimal input signal to maximize the amount of stored energy extracted from the amplifier gain medium with a fixed input energy level. ES is a non-model based real-time optimization approach for dynamic problems where only limited

[*]Correspondence author.

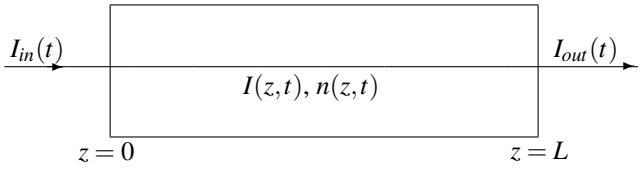

Figure 1. THE TOPOLOGY OF A SINGLE-PASS LASER AMPLIFIER.

knowledge of a system is available, such as, that the system has a nonlinear equilibrium map that has a local minimum or maximum. A popular tool in control applications in the 1940–1950s, ES has experienced a resurgence after its rigorous stability analysis was established for the first time in [9] and with further theoretical results in discrete-time systems [10]. Many successful applications of ES have been reported in the literature, including source seeking with nonholonomic unicycles in [11, 12], control of combustion instability in [13], maximizing the pressure rise in an axial flow compressor in [14] and limit cycle minimization in [15]. This work will be the first time that ES is employed in high-performance photolithography light source systems. Motivated by [16], where ES was introduced to solve noncooperative games with infinitely-many players, our problem in this paper is formulated as an infinite-dimensional optimal control problem by the parametrization of the evolution of the input pulse in the time interval $[0,T]$. The advantage of our approach is that neither the desired output nor model information is required in pulse shaping optimization via ES.

MOTION PLANNING AND OPTIMIZATION FOR SINGLE-PASS LASER MODEL

In this section, we design input signals for the single-pass laser model using ILC and ES control methods to achieve either desired or optimal pulse shapes.

PDE Model of Single-Pass Laser Dynamics

Consider the intensity dynamics of the laser beam for a single-pass model, shown in Fig. 1, which are described by a one-dimensional transport PDE system coupled with a nonlinear ODE parameterized over the spatial domain $z \in [0,L]$ and the temporal domain $t \in [0,T]$,

$$\begin{aligned}
\frac{\partial I(z,t)}{\partial t} &= -c\frac{\partial I(z,t)}{\partial z} + \sigma c n(z,t) I(z,t) - \alpha I(z,t) \\
\frac{\partial n(z,t)}{\partial t} &= -\frac{1}{F_{sat}} I(z,t) n(z,t) - \frac{1}{\tau} n(z,t) + \rho(t) \\
I(0,t) &= I_{in}(t) \qquad \text{boundary condition/input} \\
I(L,t) &= I_{out}(t) \qquad \text{boundary value/output}
\end{aligned} \tag{1}$$

Table 1. PARAMETER VALUES

L	T	c	σ	α	τ	F_{sat}
(cm)	(ns)	(m/s)	(cm^2)	(cm^{-1})	(ns)	(mJ/cm^2)
50	150	3e8	2.8e-16	0.006	1.75	3.67

where I is the density, n is the population difference between the upper and lower laser levels (in our case exactly equal to the number of ArF^* excimers), and ρ is the pumping rate (effected by glow discharge), with initial conditions specified by $I_0(z) = I(z,0)$, $n_0(z) = n(z,0)$. The parameters c, σ, α, τ, and F_{sat} are chosen in this paper as in Tab. 1.

Our objectives are the following:

(i) To find the input signal $I^r_{in}(t)$ at $z = 0$ to produce the desired output signal shape $I^r_{out}(t)$.
(ii) To find an optimal input signal to extract the maximum amount of stored energy from the amplifier gain medium.

Iterative Learning Control

Due to the complex nonlinear PDE dynamics involved in Eq. (1), it is of interest to consider non-model based methods for pulse shaping. When the system dynamics are not well known, a successful ILC scheme can improve the tracking accuracy by adjusting the system inputs from one repetition cycle to another based on the error observations in each cycle.

Given a desired output signal shape $I^r_{out}(t)$ over the period of a pulse, there are two classic ILC schemes used to achieve $I^r_{out}(t)$: proportional (P) and differential (D), which differ in their use of the iterative error function $e^k(t) = I^r_{out}(t) - I^k_{out}(t)$ as seen below:

$$\text{proportional:} \quad I^{k+1}_{in}(t) = I^k_{in}(t) + \Gamma e^k(t), \tag{2}$$

$$\text{differential:} \quad I^{k+1}_{in}(t) = I^k_{in}(t) + \Phi \dot{e}^k(t), \tag{3}$$

where k represents the iteration index, and Γ and Φ are the learning factors to be determined to generate a sequence $I^k_{out}(t)$ that converges to the desired trajectory $I^r_{out}(t)$.

To achieve better performance, we combine the P-type in (2) and D-type (3) into the following PD-type ILC scheme:

$$I^{k+1}_{in}(t) = I^k_{in}(t) + \Gamma e^k(t) + \Phi \dot{e}^k(t). \tag{4}$$

Simulation Results. Figure 2 depicts the achieved input and output signals, $I_{in}(t)$ and $I_{out}(t)$, when implementing the proposed PD-type ILC scheme, with $\Gamma = 0.08$, and $\Phi = 0.1$. It can be seen that, without a dynamical model, ILC yields, after 30 iterations, the input signal $I_{in}(t)$ that produces the desired output signal shape $I^r_{out}(t)$. Here one iteration of the ILC algorithm takes the time needed for one laser pulse (T).

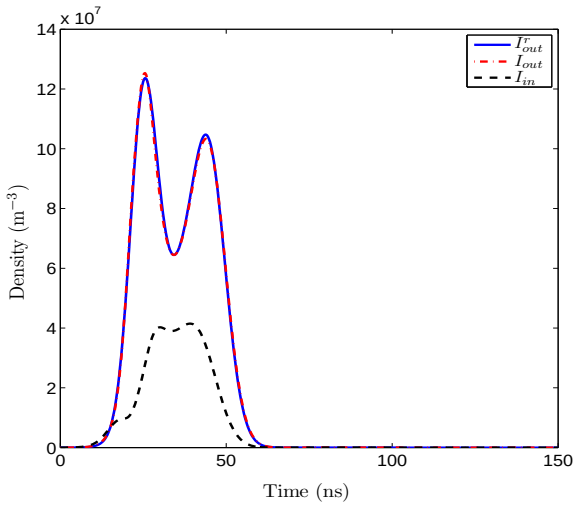

Figure 2. THE INPUT AND OUTPUT SIGNALS USING PD-TYPE ILC ALGORITHM FOR SINGLE-PASS LASER MODEL

Extremum Seeking

In this section, we proceed to optimize the input signal to extract the maximum stored energy from the amplifier gain medium while using a fixed input energy. Specifically, given the fixed input energy $\int_0^T I_{in}(t)dt$ over a period $t \in [0,T]$, we seek the optimal input pulse shape such that the output energy over a pulse $\int_0^T I_{out}(t)dt$ is maximized, i.e.,

$$\max_{I_{in}(t)\geq 0} \int_0^T I_{out}(t)dt \quad \text{subject to} \int_0^T I_{in}(t)dt \text{ fixed.} \tag{5}$$

To assure that the input energy is fixed, we modulate the input signal over the period $[0,T]$ as

$$I_{in}^{mod}(t) = \frac{I_{in}(t)}{\int_0^T I_{in}(t)dt} E_{in}^0, \tag{6}$$

where $E_{in}^0 = \int_0^T I_{in}^0(t)dt$ and $I_{in}^0(t)$ is the initial input pulse. It is impossible to solve the optimization problem (5) analytically; hence, in this paper, we explore the usage of ES, the efficient model-free optimization tool, to solve the optimization problem (5). The main idea is to parametrize the input $I_{in}(t)$ over $[0,T]$ to facilitate the application of ES.

We assume that the input pulse $I_{in}(t)$, $t \in [0,T]$ is approximated in the space $L^2[0,T]$ as follows:

$$I_{in}(t) = \sum_{j=1}^{N} \theta_j \mathbf{1}_{[t_j,t_{j+1}]}(t), \quad t \in [t_j,t_{j+1}] \tag{7}$$

where $[0,T]$ is separated into N intervals $[t_j,t_{j+1}]$, $j = 1,2,...,N$, $t_1 = 0$ and $t_{N+1} = T$, and where $\mathbf{1}_{[t_j,t_{j+1}]}(t)$ denotes the characteristic function in the interval $[t_j,t_{j+1}]$, i.e.,

$$\mathbf{1}_{[t_j,t_{j+1}]}(t) = \begin{cases} 1, \ t \in [t_j,t_{j+1}); \\ 0, \ \text{otherwise.} \end{cases} \tag{8}$$

and θ_j is the weight for the j-th characteristic function.

In practice, some constraints on the input function $I_{in}(t)$ have to be considered due to the dynamics and magnitude constraints in the electronics that generate the input signal. For example, $I_{in}(t)$ cannot be too short or too long in duration, and $I_{in}(t)$ cannot change rapidly. Therefore, we include a penalty on the input gradient in the cost function, which penalizes narrow input signals, e.g., an impulse signal. Specifically, we consider the optimization problem

$$\max_{\theta>0} J(\theta), \text{ with } J(\theta) = \frac{\int_0^T I_{out}(t)dt}{E_{in}^0} - \beta \int_0^T \dot{I}_{in}^2(t)dt, \quad \text{subject to} \int_0^T I_{in}(t)dt = E_{in}^0, \tag{9}$$

where $\beta > 0$ is the penalty weight, $\theta = [\theta_1,\theta_2,...,\theta_N]^T$ is defined in (7), and E_{in}^0 is included for scaling purposes.

The extremum seeking scheme is depicted in Fig. 3, where $\theta(k) = [\theta_1(k),\theta_2(k),...,\theta_N(k)]^T$, $\hat{\theta}(k) = [\hat{\theta}_1(k),\hat{\theta}_2(k),...,\hat{\theta}_N(k)]^T$, $a\sin\omega k$ and $a\sin(\omega k - \phi)$ are perturbation signals, with $a = [a_1,a_2,...,a_N]^T$, $\omega = [\omega_1,\omega_2,...,\omega_N]^T$, $\phi = [\phi_1,\phi_2,...,\phi_N]^T$ and $k^\theta = [k_1^\theta,k_2^\theta,...,k_N^\theta]^T$.

Simulation Results. The simulation results are shown in Figs. 4-6 for an initial input signal $I_{in}^0(t)$, which is a double-hump pulse with energy $E_{in}^0 = 1.0$ m^{-3}·s, and penalty weight $\beta = 2.25 \times 10^{-24}$ m^6·s (where we have given the penalty weight β units so that the cost J is a nondimensional value). We can observe that:

(i) The optimal cost $J^* = 3.97$ and optimal amplifier gain $E_{out}/E_{in} = 4.86$ are achieved after 2.0×10^5 ES steps (where one step of the ES algorithm takes the time needed for one laser pulse (T)).

(ii) The input pulse shape converges to an optimal single-hump pulse, whose base is widened due to the gradient penalty term.

REAL-TIME OPTIMIZATION USING EXTREMUM SEEKING FOR DOUBLE-PASS LASER MODEL

In the previous section, pulse shaping and optimization has been investigated for a single-pass model of laser systems. Practically, we are interested in the intensity dynamics of beams in multi-pass and regenerative laser amplifiers. In this section, we use ES to obtain an optimized input signal for the double-pass

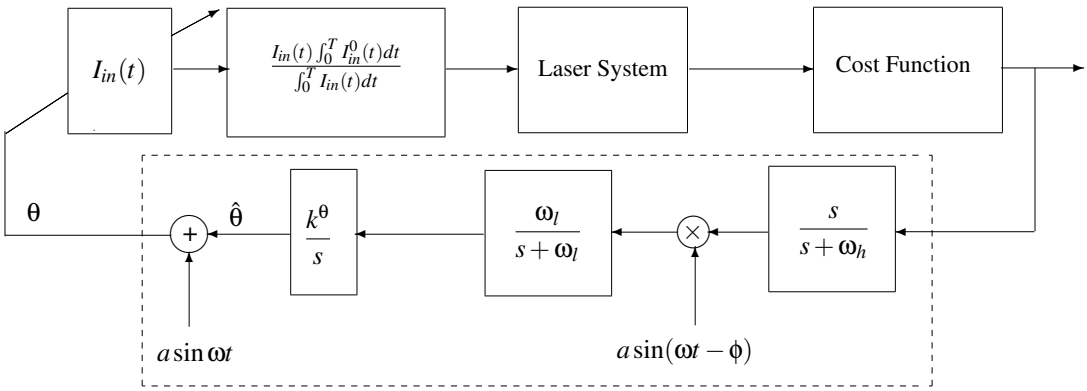

ES implemented in discrete time with step size T

Figure 3. ES SCHEME FOR INPUT PULSE SHAPING

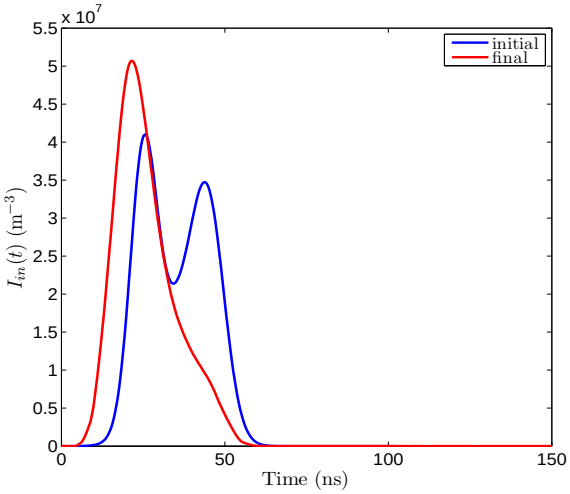

Figure 4. THE INPUT SIGNAL USING ES ALGORITHM FOR SINGLE-PASS LASER MODEL

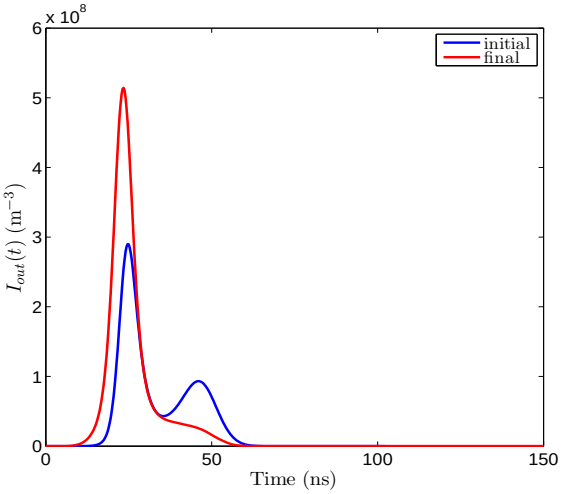

Figure 5. THE OUTPUT SIGNAL USING ES ALGORITHM FOR SINGLE-PASS LASER MODEL

model. Without loss of generality, we consider the double-pass topology as shown in Fig. 7, where we have complete overlap of the two passes.

PDE Model of Double-Pass Laser Dynamics

The intensity dynamics of the laser beam in Fig. 7 is described as follows for $z \in (0,L]$, $t \in [0,T]$:

$$\begin{aligned}
\frac{\partial I_{lr}(z,t)}{\partial t} &= -c\frac{\partial I_{lr}(z,t)}{\partial z} + \sigma c n(z,t) I_{lr}(x,t) - \alpha I_{lr}(z,t) \\
\frac{\partial I_{rl}(z,t)}{\partial t} &= c\frac{\partial I_{rl}(z,t)}{\partial z} + \sigma c n(z,t) I_{rl}(z,t) - \alpha I_{rl}(z,t) \\
\frac{\partial n(z,t)}{\partial t} &= -\frac{1}{F_{sat}}\Big[I_{lr}(z,t) + I_{rl}(z,t)\Big] n(z,t) - \frac{1}{\tau} n(z,t) + \rho(t)
\end{aligned} \tag{10}$$

with boundary conditions,

$$\begin{aligned}
I_{lr}(0,t) &= I_{in}(t), \quad \text{boundary condition/input,} \\
I_{rl}(L,t) &= I_{lr}(L,t), \text{ boundary condition,} \\
I_{rl}(0,t) &= I_{out}(t), \quad \text{boundary value/output,}
\end{aligned} \tag{11}$$

where I_{lr} and I_{rl} are the rightward and leftward density respectively, n is the population difference between the upper and lower laser levels, and ρ is the pumping rate, with initial conditions $I_{lr}(z,0) = I_{lr}^0(x)$, $I_{rl}(z,0) = I_{rl}^0(x)$, $n(z,0) = n^0(x)$.

Figure 8 shows the input-output relationship for the double-pass laser system in Eqs. (10)–(11). It can be seen that the double-pass output $I_{out}(t) = I_{rl}(0,t)$ is amplified compared to the single-pass output $I_{lr}(L,t)$ with the input signal $I_{in}(t) = I_{lr}(0,t)$. Therefore, the double-pass model allows for more efficient en-

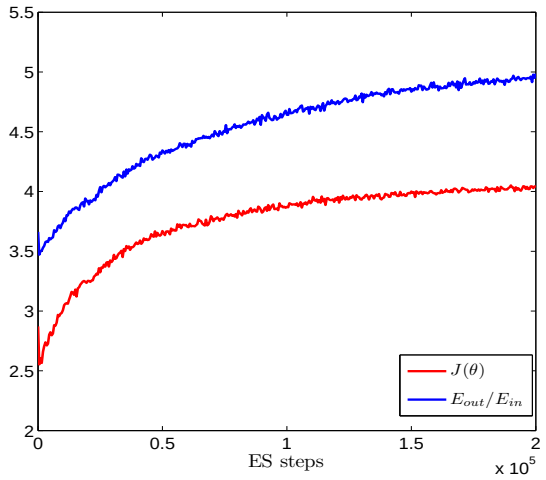

Figure 6. THE COST FUNCTION AND AMPLIFIER GAIN USING ES ALGORITHM FOR SINGLE-PASS LASER MODEL

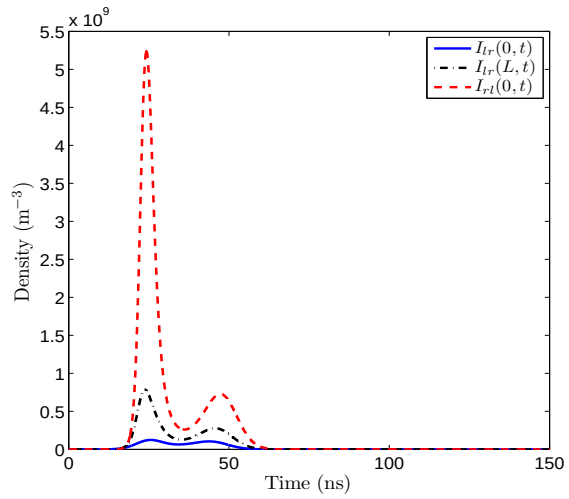

Figure 8. INPUT AND OUTPUT SIGNALS OF DOUBLE-PASS LASER MODEL.

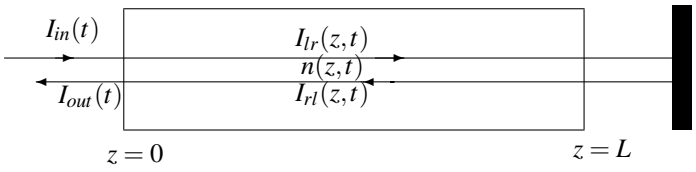

Figure 7. DOUBLE-PASS LASER AMPLIFIER WITH COMPLETE OVERLAP OF THE TWO PASSES.

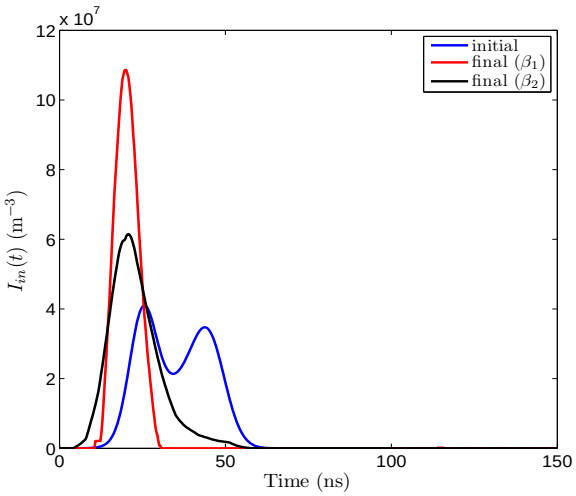

Figure 9. THE INPUT SIGNAL USING ES ALGORITHM FOR THE DOUBLE-PASS LASER MODEL.

ergy extraction.

Optimization of Input Pulse Using ES

Similar to the single-pass model case, we employ ES to solve the optimization problem (9) for the double-pass model, i.e., seek the optimal input pulse shape for maximizing the extraction energy.

Simulation Results. Figures 9 and 10 depict the initial and final signal pulse shapes for the input $I_{in}(t)$ and the output $I_{out}(t)$ signals, and Figs. 11 and 12 show the evolution of the cost $J(\theta)$ and amplifier gain E_{out}/E_{in}.

For fixed input energy $E_{in} = 1.0$ m^{-3}·s,

(i) the input pulse converges to an optimal single-hump pulse,
(ii) the duration of the pulse increases, i.e., its rate of change decreases, and its peak value decreases as β is increased,
(iii) the achieved amplifier gain and ES convergence rate both decrease as β is increased, and
(iv) compared to the results for the single-pass laser system with $\beta = 2.25 \times 10^{-24}$ m^6·s, the optimized amplifier gain increases from 4.86 to 38.83.

Examining the two scenarios more closely, we have when $\beta = 2.25 \times 10^{-24}$ m^6·s, the optimal cost $J^* = 31.92$ and optimized amplifier gain $E_{out}/E_{in} = 38.83$ are achieved after 4×10^4 ES steps; and when $\beta = 6.75 \times 10^{-24}$ m^6·s, the optimal cost $J^* = 21.62$ and optimized amplifier gain $E_{out}/E_{in} = 28.49$ are achieved after 1×10^5 ES steps.

Optimization of Both Input Pulse and Pumping Rate Using ES

So far, ES has been used to optimize the input pulse $I_{in}(t)$ with the pumping rate $\rho(t)$ given. It is interesting to investigate optimizing both $I_{in}(t)$ and $\rho(t)$ using ES to maximize the extrac-

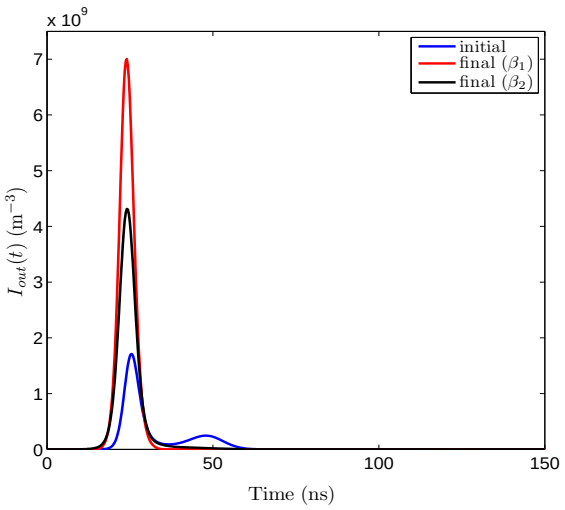

Figure 10. THE OUTPUT SIGNAL USING ES ALGORITHM FOR THE DOUBLE-PASS LASER MODEL.

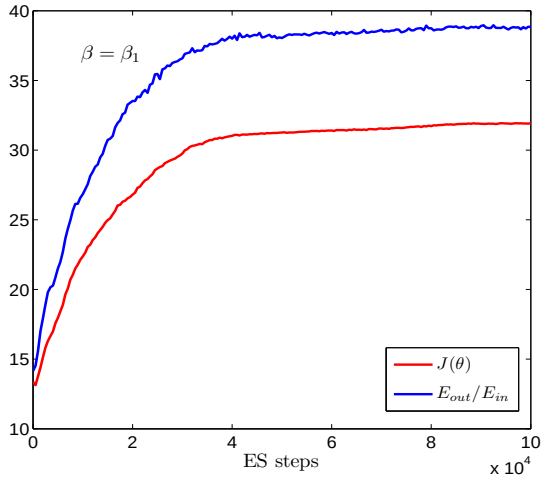

Figure 11. THE COST FUNCTION USING ES ALGORITHM FOR THE DOUBLE-PASS LASER MODEL.

tion of the stored energy from the amplifier gain medium.

We assume that the input pulse $I_{in}(t)$ and pumping rate $\rho(t)$, $t \in [0,T]$, are approximated in the space $L^2[0,T]$ as follows:

$$I_{in}(t) = \sum_{j=1}^{N} \theta_j^I \mathbf{1}_{[t_j,t_{j+1}]}(t), \quad t \in [t_j,t_{j+1}] \tag{12}$$

$$\rho(t) = \sum_{j=1}^{N} \theta_j^\rho \mathbf{1}_{[t_j,t_{j+1}]}(t), \quad t \in [t_j,t_{j+1}] \tag{13}$$

where $[0,T]$ is separated into N intervals $[t_j,t_{j+1}]$, $j = 1,2,...,N$, $t_1 = 0$ and $t_{N+1} = T$, and where $\mathbf{1}_{[t_j,t_{j+1}]}(t)$ denotes the characteristic function given by (8). The weights for the j-th characteristic

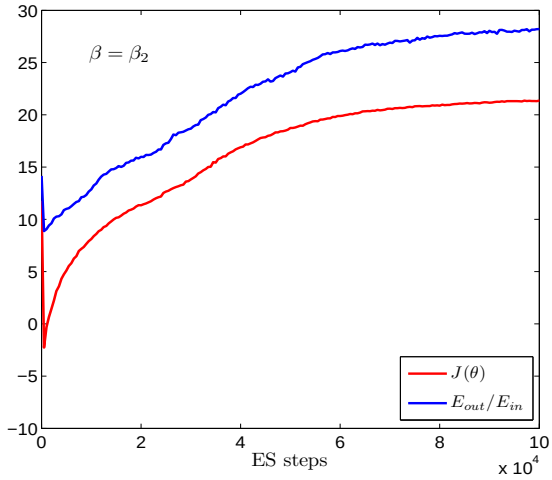

Figure 12. THE AMPLIFIER GAIN USING ES ALGORITHM FOR THE DOUBLE-PASS LASER MODEL.

function of $I_{in}(t)$ and $\rho(t)$ are denoted by θ_j^I and θ_j^ρ, respectively.

Due to practical constraints on the input function $I_{in}(t)$ and the pumping rate $\rho(t)$, we include both a penalty on the input gradient and a penalty on the pumping rate gradient in the cost function to prevent $I_{in}(t)$ and $\rho(t)$ from having a rapid rate of change or gradient. Hence, the optimization problem becomes

$$\max_{\theta^I>0,\theta^\rho>0} J(\theta^I,\theta^\rho), \tag{14}$$

$$\text{with } J(\theta^I,\theta^\rho) = \frac{\int_0^T I_{out}(t)dt}{E_{in}^0} - \beta\int_0^T \dot{I}_{in}^2(t)dt - \gamma\int_0^T \dot{\rho}^2(t)dt,$$

$$\text{subject to } \int_0^T I_{in}(t)dt = E_{in}^0, \ \int_0^T \rho(t)dt = V_\rho^0.$$

where $\beta > 0$ and $\gamma > 0$ are the penalty weights for the input gradient and the pumping rate gradient, $\theta^I = [\theta_1^I,\theta_2^I,...,\theta_N^I]^T$ and $\theta^\rho = [\theta_1^\rho,\theta_2^\rho,...,\theta_N^\rho]^T$, which are defined in (12) and (13), and $V_\rho^0 = \int_0^T \rho^0(t)\,dt$.

The ES scheme is depicted in Fig. 13, where $\theta^I(k)$ and $\theta^\rho(k)$ are the weight vectors of $I_{in}(t)$ and $\rho(t)$ to be optimized; $\hat{\theta}^I(k)$ and $\hat{\theta}^\rho(k)$ are the estimates of $\theta^I(k)$ and $\theta^\rho(k)$, respectively; and $a^I\sin\omega^I k$, $a^I\sin(\omega^I k - \phi^I)$, $a^\rho\sin\omega^\rho k$ and $a^\rho\sin(\omega^\rho k - \phi^\rho)$ are perturbation signals.

Simulation Results. Figures 14-16 show the initial and final signal pulse shapes for the input $I_{in}(t)$, pumping rate $\rho(t)$, and $I_{out}(t)$ signals respectively. The evolution of the cost $J(\theta^I,\theta^\rho)$ and amplifier gain E_{out}/E_{in} is also shown in Fig. 17.

For the fixed input energy $E_{in} = 1.0$ m^{-3}·s, pumping volume $V_\rho = 3.0\times10^{21}$ m^{-3} and penalty weights $\beta = 3.75\times10^{-24}$m^6·s, $\gamma = 2.4\times10^{-67}$ m^6·s^3,

(i) the optimal cost $J^* = 596.55$ and optimal amplifier gain $E_{out}/E_{in} = 810.71$ are achieved after 3×10^5 ES steps,

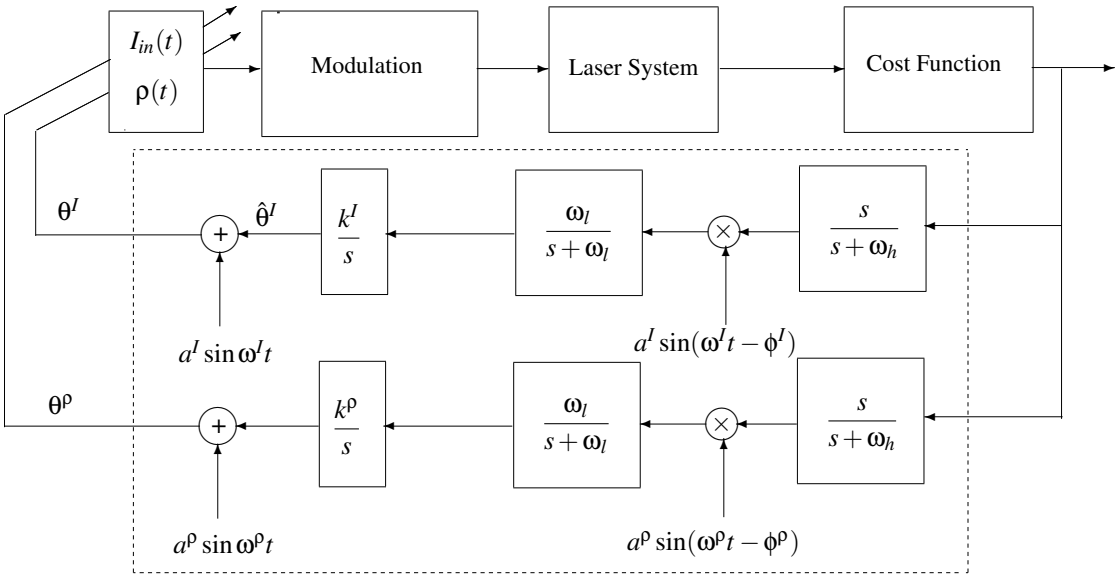

Figure 13. ES SCHEME FOR BOTH INPUT PULSE SHAPING AND PUMPING RATE PULSE SHAPING.

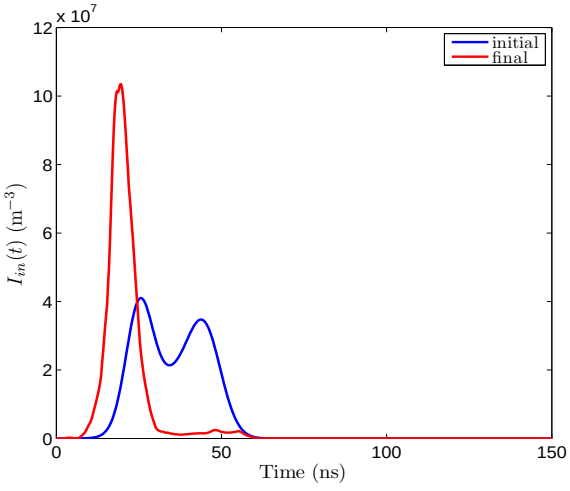

Figure 14. THE INITIAL AND FINAL INPUT SIGNAL USING ES FOR DOUBLE-PASS LASER MODEL WHEN OPTIMIZING BOTH INPUT AND PUMPING RATE.

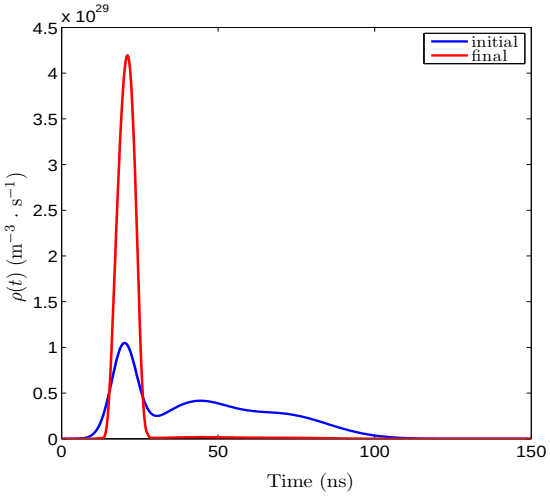

Figure 15. THE INITIAL AND FINAL PUMPING RATE USING ES FOR DOUBLE-PASS LASER MODEL WHEN OPTIMIZING BOTH INPUT AND PUMPING RATE.

(ii) the input pulse converges from a double-hump pulse to an optimal single-hump pulse,
(iii) the pumping rate pulse also converges to an optimal single-hump pulse, and
(iv) compared with the ES results for the double-pass laser model when the pumping rate $\rho(t)$ is a given value, the energy amplifier gain is increased from 38.83 to 810.71.

CONCLUSIONS AND FUTURE WORK

In this paper we have investigated the design of the shape of laser pulses for both single-pass model and double-pass model to achieve desired, or optimal, pulse shapes, through learning-based and optimization-based tools. The effectiveness of these control designs has been verified via numerical simulations. In future work, efforts will be placed on the modeling, design and

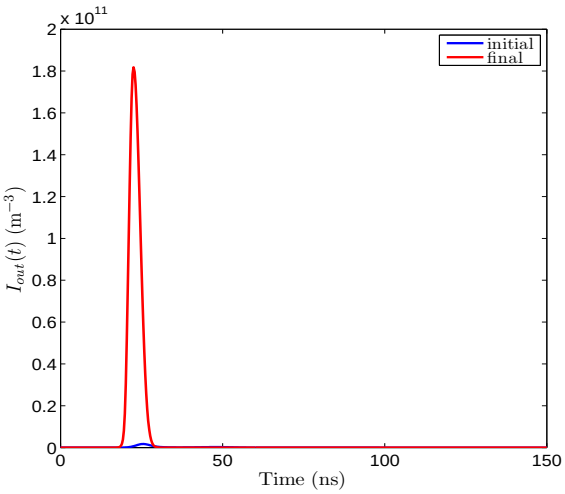

Figure 16. THE INITIAL AND FINAL OUTPUT SIGNAL USING ES FOR DOUBLE-PASS LASER MODEL WHEN OPTIMIZING BOTH INPUT AND PUMPING RATE.

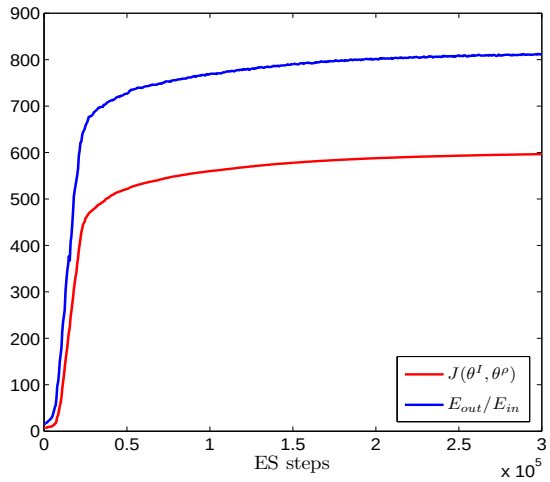

Figure 17. THE COST FUNCTION AND AMPLIFIER GAIN FOR DOUBLE-PASS LASER MODEL WHEN OPTIMIZING BOTH INPUT AND PUMPING RATE.

validation of the case when optical feedback in the amplifier is used. This setup allows for more efficient energy extraction and a longer output pulse length.

REFERENCES

[1] Frantz, L. M., and Nodvik, J. S., 1963. "Theory of pulse propogation in a laser amplifier". *Journal of Applied Physics,* **34**(8), pp. 2346–2349.

[2] Akashi, H., Sakai, Y., and Tagashira, H., 1995. "Modelling of a self-sustained discharge-excieted arf excimer laser: the influence of photo-ionization and photodetachment by laser light on the discharge development". *J. Phys. D: Appl. Phys.,* **28**, pp. 445–451.

[3] Moore, K. L., 1993. *Iterative Learning Control of Deterministic System*. Springer-Verlag, New York.

[4] Chen, Y., and Wen, C., 1999. *Iterative Learning Control: Robustness and Applications*. Springer, New York.

[5] Xu, J., and Tan, Y., 2003. *Linar and Nonlinear Iterative Learning Control*. Springer, New York.

[6] Qu, Z., 2002. "An iterative learning algorithm for boundary control of a stretched moving string". *Automatica,* **38**, pp. 821–827.

[7] Xu, C., Arastoo, R., and Schuster, E., 2009. "On iterative learning control of parabolic distributed parameter systems". In Proc. 17th Mediterranean Conference on Control & Automation, pp. 510–515.

[8] Ariyur, K., and Krstić, M., 2003. *Real-Time Optimization by Extremum Seeking Control*. Wiley-Interscience, Hoboken, NJ.

[9] Krstić, M., and Wang, H. H., 2000. "Stability of extremum seeking feedback for general nonlinear dynamic systems". *Automatica,* **36**, pp. 595–601.

[10] Choi, J.-Y., Krstić, M., Ariyur, K. B., and Lee, J. S., 2002. "Extremum seeking control for discrete-time systems". *IEEE Trans. Automat. Contr.,* **47**, pp. 318–323.

[11] Zhang, C., Arnold, D., Ghods, N., Siranosian, A., and Krstić, M., 2007. "Source seeking with nonholonomic unicycle without position measurement and with tuning of forward velocity". *Systems & Control Letters,* **56**, pp. 245–252.

[12] Cochran, J., Kanso, E., Kelly, S. D., Xiong, H., and Krstić, M., 2009. "Source seeking for two nonholonomic models of fish locomotion". *IEEE Trans. Robot. Automat.,* **25**, pp. 1166–1176.

[13] A. Banaszuk, K. B. Ariyur, M. K., and Jacobson, C. A., 2004. "An adaptive algorithm for control of combustion instability". *Automatica,* **40**, pp. 1965–1972.

[14] Wang, H.-H., Yeung, S., and Krstić, M., 2000. "Experimental application of extremum seeking on an axial-flow compressor". *IEEE Trans. Contr. Syst. Technol.,* **8**, pp. 300–309.

[15] Wang, H.-H., and Krstić, M., 2000. "Extremum seeking for limit cycle minimization". *IEEE Trans. Robot. Automat.,* **45**, pp. 2432–2437.

[16] Frihauf, P., Krstić, M., and Basar, T., 2011, to appear. "Nash equilibrium seeking with infinitely many players". *2011 American Control Conference*.